Stability Analysis of a Thick Plate with Interior Cutout

Chiang-Nan Chang*
National Central University, Chung-Li, Taiwan
and
Feung-Kung Chiang†
Tsi-Hai Institute of Technology, Taipei, Taiwan

Plates with interior cutout are often used in industrial design such as machines, bridges, aircraft, etc. Many advantages, such as reduced weights, easy access for maintenance, and easier assembling process, can be obtained by the design. However, when interior holds were cut from plate structures, mechanical behaviors of the structures were changed. To avoid structure instability, buckling behavior of such plate structures must be studied. The current research studies the buckling behavior of Mindlin-thick plates with interior cutout for different boundaries and different opening ratios. An incremental deformation concept is adapted and the curvature effect is considered. The quadratic element of the eight node is used. Selective-reduced integration is used to find integration of the stiffness matrix. Eigenvalues and eigenvectors are calculated by the subspace iteration method. The validity of the calculations are checked out against existing solutions for full-plate buckling. It is shown that opening ratios have different effects on buckling for different boundary conditions.

Introduction

TRADITIONAL buckling analysis used classical beam or plate theory, which is not satisfactory when rotary inertia and/or transverse shear become important. Sun, in 1972,[1] studied the buckling of a Timoshenko beam under initial stress. In the same year, Brunelle studied the stability and vibration problem of a transversely isotropic, prestressed Timoshenko beam.[2] Herrmann used the Mindlin-thick plate theory to handle stability of a plate under initial stress.[3] Brunelle and Robertson[4] used the average stresses and variational method to study stability of a uniformly prestressed plate. The variational method in his study is similar to Herrmann, but the method has an extra curvature term. Hinton[5] used the finite-strip method; while Dawe[6] used the Rayleigh-Ritz and finite strip methods to handle different boundary conditions. Cheung[7] used the finite element to solve linear elastic plate buckling. His study showed that the curvature effect is not important for thin plate. Paramasivam[8] used a discrete model to solve square-plate buckling with abruptly varying stiffness. Mizusawa[9] used B-Spline and Rayleigh-Ritz to study stability and vibration of plates with discontinuous, varying stiffness. Tham[10] used the negative stiffness method to work on discontinuous stiffness problems. His results agreed quite well with other people's work.

Despite the intensive study of full plate, few buckling analyses about plates with interior cutout were found in literature. The primary interest of this research is to investigate stability of plates with interior cutout. A well-established, finite, element model was used. Different boundary conditions for both inside and outside edges are considered. Interesting results are obtained which were not previously known.

Theoretical Background

Mindlin, in 1951, published the famous thick-plate theory. This two-dimensional theory of flexural motions of isotropic, elastic plate is deduced from the three-dimensional equations of elasticity. The theory includes the effects of rotatory inertia and shear in the same manner as Timoshenko's one-dimensional theory of bars. The following assumptions are also applied.

1) The straight line that is vertical to the neutral surface before deformation remains straight but not necessarily vertical to the neutral surface after deformation.

2) Displacement is small so that small deformation theory can be applied.

3) Normal stress in the z direction is neglected.

4) Body force is neglected.

Consider a plate cross section as shown in Fig. 1. Cartesian coordinates x,y,z are fixed on the neutral surface of the plate before deformation. Displacement along the x,y,z direction is

$$u(x,y,z) = -z\theta_x(x,y) \tag{1a}$$

$$v(x,y,z) = -z\theta_y(x,y) \tag{1b}$$

$$w(x,y,z) = w(x,y) \tag{1c}$$

Assume the plate is subject to initial stress r_x^0, r_y^0 in x,y directions, respectively, and τ_{xy}^0 along the outside edges. Let the prestressed state be the initial state. Then, the higher-order terms of γ_{xz} and γ_{yz} can be neglected if small lateral deflection is assumed and the incremental stress concept is used. The

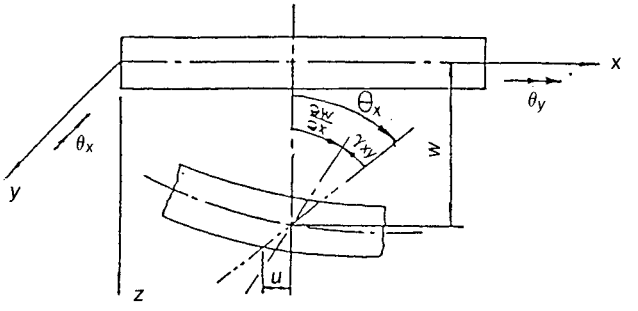

Fig. 1 Thick plate deformation and coordinates.

Received May 11, 1989; revision received July 10, 1989;

*Associate Professor, Department of Mechanical Engineering.
†Lecturer.

finite strain vector can then be reduced to the following.

$$\begin{Bmatrix} \epsilon_x \\ \epsilon_y \\ \gamma_{xy} \\ \gamma_{xx} \\ \gamma_{yz} \end{Bmatrix} = \begin{Bmatrix} \dfrac{\partial u}{\partial x} \\ \dfrac{\partial v}{\partial y} \\ \dfrac{\partial u}{\partial y} + \dfrac{\partial v}{\partial x} \\ \dfrac{\partial w}{\partial x} + \dfrac{\partial u}{\partial z} \\ \dfrac{\partial w}{\partial y} + \dfrac{\partial v}{\partial z} \end{Bmatrix} + \begin{Bmatrix} \dfrac{1}{2}\left[\left(\dfrac{\partial u}{\partial x}\right)^2 + \left(\dfrac{\partial v}{\partial x}\right)^2 + \left(\dfrac{\partial w}{\partial x}\right)^2\right] \\ \dfrac{1}{2}\left[\left(\dfrac{\partial u}{\partial y}\right)^2 + \left(\dfrac{\partial v}{\partial y}\right)^2 + \left(\dfrac{\partial w}{\partial y}\right)^2\right] \\ \left(\dfrac{\partial u}{\partial x}\right)\left(\dfrac{\partial u}{\partial y}\right) + \left(\dfrac{\partial v}{\partial x}\right)\left(\dfrac{\partial v}{\partial y}\right) + \left(\dfrac{\partial w}{\partial x}\right)\left(\dfrac{\partial w}{\partial y}\right) \\ 0 \\ 0 \end{Bmatrix} \tag{2}$$

Equation (2) includes linear and nonlinear terms and can be abbreviated as

$$\{\epsilon\} = \{\epsilon^L\} + \{\epsilon^{nL}\}$$

where

ϵ: total strain

ϵ^L: linear strain

ϵ^{nL}: nonlinear strain

The two-dimensional equation can be written as

$$\begin{Bmatrix} \bar{t}_x \\ \bar{t}_y \\ \bar{t}_{xy} \\ \bar{t}_{xx} \\ \bar{t}_{ux} \end{Bmatrix} \quad \begin{Bmatrix} \sigma_x \\ \sigma_y \\ \tau_{xy} \\ \tau_{xx} \\ \tau_{yz} \end{Bmatrix} \quad \begin{Bmatrix} \sigma_x^0 \\ \sigma_y^0 \\ \tau_{xy}^0 \\ 0 \\ 0 \end{Bmatrix}$$

or abbreviated as

$$\{\bar{t}\} = \{\sigma\} + \{\sigma^0\}$$

where

$\bar{t}$: final stress

σ: incremental stress

σ^0: initial stress

For homogeneous, isotropic plate, stress strain relation in matrix form is

$$\{\sigma\} = [C]\,\{\epsilon\}$$

Where

$$[C] = \begin{bmatrix} E & \nu E & & & \\ \nu E & E & & & 0 \\ & & G & & \\ 0 & & & G & \\ & & & & G \end{bmatrix}$$

Strain energy in unit volume is

$$\begin{aligned} V_1 &= \{\sigma^0\}^T\{\epsilon\} + \frac{1}{2}\{\sigma\}^T\{\epsilon\} \\ &= \{\sigma^0\}^T\{\epsilon\} + \frac{1}{2}\{\epsilon\}^T[C]\{\epsilon\} \\ &= \{\sigma^0\}^T\{\epsilon^L\} + \{\sigma^0\}^T\{\epsilon^{nL}\} + \frac{1}{2}\{\epsilon^L\}^T[C]\{\epsilon^L\} \\ &\quad + \frac{1}{2}\{\epsilon^L\}^T[C]\{\epsilon^{nL}\} + \frac{1}{2}\{\epsilon^{nL}\}^T[C]\{\epsilon^L\} \\ &\quad + \frac{1}{2}\{\epsilon^{nL}\}^T[C]\{\epsilon^{nL}\} \end{aligned} \tag{3}$$

Neglect third and higher-order terms for displacement gradient, and Eq. (3) can be simplified:

$$U_1 = \{\sigma^0\}^T\{\epsilon^L\} + \{\sigma^0\}^T\{\epsilon^{nL}\} + \frac{1}{2}\{\epsilon^L\}^T[C]\{\epsilon^L\}$$

Incremental strain energy can be derived as follows:

$$\begin{aligned} \Delta U_I &= U_I - \{\sigma^0\}^T\{\epsilon^L\} \\ &= \{\sigma^0\}^T\{\epsilon^{nL}\} + \frac{1}{2}\{\epsilon^L\}^T[C]\{\epsilon^L\} \\ &= \frac{1}{2}\{\epsilon^L\}^T[C]\{\epsilon^L\} + \frac{1}{2}\sigma_x^0\left[z^2\left(\frac{\partial\theta_x}{\partial x}\right)^2 + z^2\left(\frac{\partial\theta_y}{\partial x}\right)^2 + \left(\frac{\partial w}{\partial x}\right)^2\right] + \frac{1}{2}\sigma_y^0\left[z^2\left(\frac{\partial\theta_x}{\partial y}\right)^2 + z^2\left(\frac{\partial\theta_y}{\partial y}\right)^2 + \left(\frac{\partial w}{\partial y}\right)^2\right] \\ &\quad + \tau_{xr}^0\left[z^2\left(\frac{\partial\theta_x}{\partial x}\right)\left(\frac{\partial\theta_x}{\partial y}\right) + z^2\left(\frac{\partial\theta_y}{\partial x}\right)\left(\frac{\partial\theta_y}{\partial y}\right) + \left(\frac{\partial w}{\partial x}\right)\left(\frac{\partial w}{\partial y}\right)\right] \end{aligned}$$

Perform integration with respect to z from $-h/2$ to $h/2$ and rearrange:

$$\begin{aligned} \Delta U_{LA} &= \frac{1}{2}\int_{-h/2}^{h/2}\{\epsilon^L\}^T[C]\{\epsilon^L\}\,dz + \frac{h}{2}\left[\sigma_x^0\left(\frac{\partial w}{\partial x}\right)^2 + \sigma_y^0\left(\frac{\partial w}{\partial y}\right)^2 + 2\tau_{xy}^0\left(\frac{\partial w}{\partial x}\right)\left(\frac{\partial w}{\partial y}\right)\right] + \frac{h^3}{24}\left\{\sigma_x^0\left[\left(\frac{\partial\theta_x}{\partial x}\right)^2 + \left(\frac{\partial\theta_y}{\partial x}\right)^2\right] + \sigma_y^0\left[\left(\frac{\partial\theta_x}{\partial y}\right)^2 + \left(\frac{\partial\theta y}{\partial y}\right)^2\right] + 2\tau_{xy}^0\left(\frac{\partial\theta_x}{\partial x}\right)\left(\frac{\partial\theta_x}{\partial y}\right) \right. \\ &\quad \left. + 2\tau_{xy}^0\left(\frac{\partial\theta_y}{\partial x}\right)\left(\frac{\partial\theta_y}{\partial y}\right)\right\} \end{aligned} \tag{4}$$

Let

$$Nx = \int_{-h/2}^{h/2} \sigma_x^0 \, dz = \sigma_x^0 h$$

$$Ny = \int_{-h/2}^{h/2} \sigma_y^0 = dz = \sigma_y^0 h$$

$$Nxy = \int_{-h/2}^{h/2} \tau_{xy}^0 \, dz = \tau_{xy}^0 h$$

Eq. (4) becomes

$$U_{IA} = \frac{1}{2}\int_{-h/2}^{h/2} \{\epsilon^L\}^T [C] \{\epsilon^L\} \, dz + \frac{1}{2}\left[Nx\left(\frac{\partial w}{\partial x}\right)^2 + Ny\left(\frac{\partial w}{\partial y}\right)^2 + 2Nxy\left(\frac{\partial w}{\partial x}\right)\left(\frac{\partial w}{\partial y}\right)\right] + \frac{h^2}{24}\left\{Nx\left[\left(\frac{\partial \theta_x}{\partial x}\right)^2 + \left(\frac{\partial \theta_y}{\partial x}\right)^2\right] + Ny\left[\left(\frac{\partial \theta_x}{\partial y}\right)^2 + \left(\frac{\partial \theta_y}{\partial y}\right)^2\right] + 2Nxy\left(\frac{\partial \theta_x}{\partial x}\right)\left(\frac{\partial \theta_x}{\partial y}\right) + 2Nxy\left(\frac{\partial \theta_y}{\partial x}\right)\left(\frac{\partial \theta_y}{\partial y}\right) \quad (5)$$

Total incremental strain energy can be obtained by performing integration of Eq. (5) through the neutral surface

$$\Delta U_{IC} = \iint_A \Delta U_{IA} \, dA = \iint_A \Delta U_{IA} \, dx dy$$

$$= \iint_A \frac{1}{2}\left\{D\left[\left(\frac{\partial \theta_x}{\partial x}\right)^2 + \left(\frac{\partial \theta y}{\partial y}\right)^2 + 2\nu\left(\frac{\partial \theta_x}{\partial x}\right)\left(\frac{\partial \theta_y}{\partial y}\right)\right] + \frac{Gh^3}{12}\left(\frac{\partial \theta_x}{\partial y} + \frac{\partial \theta_y}{\partial x}\right)^2 + G\hat{k}h\left(\frac{\partial w}{\partial x} - \theta_x\right)^2 + G\hat{k}h\left(\frac{\partial w}{\partial y} - \theta_y\right)^2\right\} + \frac{1}{2}\left[Nx\left(\frac{\partial w}{\partial x}\right)^2 + Ny\left(\frac{\partial w}{\partial y}\right)^2 + 2Nxy\left(\frac{\partial w}{\partial x}\right)\left(\frac{\partial w}{\partial y}\right)\right] + \frac{h^2}{24}\left\{Nx\left[\left(\frac{\partial \theta_x}{\partial x}\right)^2 + \left(\frac{\partial \theta_y}{\partial x}\right)^2\right] + Ny\left[\left(\frac{\partial \theta_x}{\partial y}\right)^2 + \left(\frac{\partial \theta_y}{\partial y}\right)^2\right] Nxy\left(\frac{\partial \theta_x}{\partial x}\right)\left(\frac{\partial \theta_x}{\partial y}\right) + 2\,Nxy\left(\frac{\partial \theta_y}{\partial x}\right)\left(\frac{\partial \theta y}{\partial y}\right)\right\} dx dy \quad (6)$$

The main difference between this governing equation and the classical plate-buckling equation is that the second-order terms are retained.

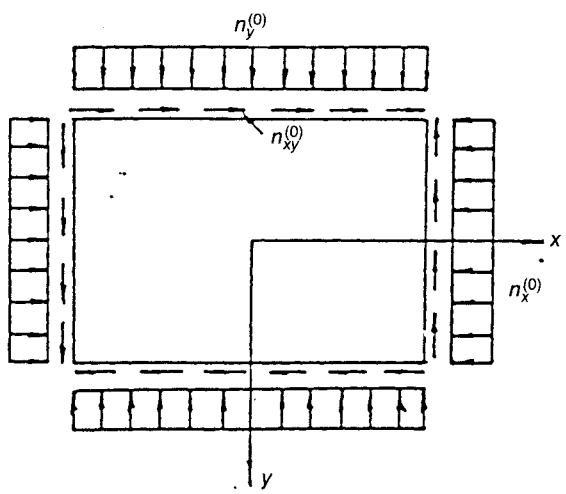

Fig. 2 Initial stresses on a rectangular plate.

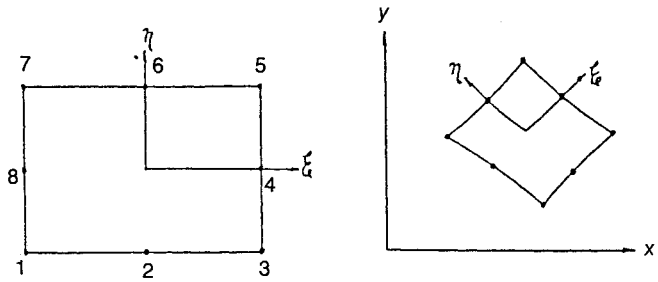

Fig. 3 Quadratic (serendipity) element.

Figure 2 shows a square plate subject to initial normal and shear stress $n_x^{(0)}$, $n_y^{(0)}$, $n_{xy}^{(0)}$.
Define buckling parameter $\lambda_b = N_{CY}b^2/\pi^2 D$, $D = Eh^3/12(1-\nu^2)$ then, we have

$$Nx = \lambda_b n_x^{(0)}$$

$$Ny = -\lambda_b n_y^{(0)}$$

$$Nxy = -\lambda_b n_{xy}^{(0)}$$

Where

N_{CY}: critical buckling load

b: plate span

To satisfy equilibrium, we have

$$\frac{\partial Nx}{\partial x} + \frac{\partial Nxy}{\partial y} = \theta$$

$$\frac{\partial Nxy}{\partial x} + \frac{\partial Ny}{\partial y} = \theta$$

$$\frac{\partial n_x^{(0)}}{\partial x} + \frac{\partial n_{xy}^{(0)}}{\partial y} = \theta$$

$$\frac{\partial n_{xy}^{(0)}}{\partial x} + \frac{\partial n_y^{(0)}}{\partial y} = \theta$$

The governing equation hence becomes

$$\Delta U_{IC} = \iint_A \frac{1}{2}\left\{D\left[\left(\frac{\partial \theta_x}{\partial x}\right)^2 + \left(\frac{\partial \theta_y}{\partial y}\right)^2 + 2\nu\left(\frac{\partial \theta_x}{\partial x}\right)\left(\frac{\partial \theta_y}{\partial y}\right)\right] + \frac{Gh^3}{12}\left(\frac{\partial \theta_x}{\partial y} + \frac{\partial \theta_y}{\partial x}\right)^2 + G\hat{k}h\left(\frac{\partial w}{\partial x} - \theta_x\right)^2 + G\hat{k}h\left(\frac{\partial w}{\partial y} - \theta_y\right)^2\right\} - \lambda_b \frac{1}{2}\left[n_x^{(0)}\left(\frac{\partial w}{\partial x}\right)^2 + n_y^{(0)}\left(\frac{\partial w}{\partial x}\right)^2 + 2n_{xy}^{(0)}\left(\frac{\partial w}{\partial x}\right)\left(\frac{\partial w}{\partial y}\right)\right] + \frac{h^2}{24}\left(n_x^{(0)}\left[\left(\frac{\partial \theta_x}{\partial x}\right)^2 + \left(\frac{\partial \theta_y}{\partial x}\right)^2\right] n_{xy}^{(0)}\left(\frac{\partial \theta_x}{\partial y}\right)\left(\frac{\partial \theta_x}{\partial x}\right) + 2n_{xy}^{(0)}\left(\frac{\partial \theta_y}{\partial x}\right)\left(\frac{\partial \theta_y}{\partial y}\right)\right\} dx dy \quad (7)$$

Finite Element Model for Mindlin Plate

Figure 3 shows a typical quadratic element (also called serendipity element). There are 8 nodes as shown in the figure. The (ξ,η) are the nondimensional local coordinates and its origin located at the center of the element. Shape functions can be expressed as follows:

Corner Nodes

$$N_i^{(e)} = \frac{1}{4}(1 + \xi\xi_i)(1 + \eta\eta_i)(\xi\xi_i + \eta\eta_i - 1)$$

$i = 1,3,5,7$

Midpoint Nodes

$$N_i^{(e)} = \frac{\xi_i^2}{2}(1+\xi\xi_i)(1-\eta^2) + \frac{\eta_i^2}{2}(1+\eta\eta_i)(1-\xi^2)$$

$$i = 2,4,6,8$$

where $-1 \le \xi \le 1$, $-1 \le \eta \le 1$. For an arbitrarily point (x,y) within an element, (x,y) can be expressed as a linear combination of shape function and nodal coordinates.

$$X = \sum_{i=1}^{n} N_i X_i$$

$$Y = \sum_{i=1}^{n} N_i X_i$$

Apply variational operation on Eq. (7). Express δw, $\delta\theta_x$, and $\delta\theta_y$ as linear combination of shape functions and modal values. Governing equations in matrix form can then be obtained:

$$\begin{bmatrix} [K^{11}] & [K^{12}] & [K^{13}] \\ & [K^{22}] & [K^{23}] \\ \text{Symm} & & [K^{33}] \end{bmatrix} \begin{Bmatrix} \{w\} \\ \{\theta_x\} \\ \{\theta_y\} \end{Bmatrix} = \lambda_b \begin{bmatrix} [G^{11}] & [G^{12}] & [G^{13}] \\ & [G^{22}] & [G^{23}] \\ \text{Symm} & & [G^{33}] \end{bmatrix} \begin{Bmatrix} \{w\} \\ \{\theta_x\} \\ \{\theta_y\} \end{Bmatrix} \tag{8}$$

where

$$K_{ij}^{11} = G\hat{k}h \iint_A \left(\frac{\partial N_i}{\partial x}\frac{\partial N_j}{\partial x} + \frac{\partial N_i}{\partial y}\frac{\partial N_j}{\partial y}\right) dxdy$$

$$K_{ij}^{12} = -G\hat{k}h \iint_A \left(\frac{\partial N_i}{\partial x} N\right) dxdy$$

$$K_{ij}^{13} = -G\hat{k}h \iint_A \left(\frac{\partial N_i}{\partial y} N\right) dxdy$$

$$K_{ij}^{22} = \iint_A \left(D\frac{\partial N_i}{\partial x}\frac{\partial N_j}{\partial x} + \frac{Gh^3}{12}\frac{\partial N_i}{\partial y}\frac{\partial N_j}{\partial y} + G\hat{k}h\, N_i N_j\right) dxdy$$

$$K_{ij}^{23} = \iint_A \left(\nu D\frac{\partial N_i}{\partial x}\frac{\partial N_j}{\partial x} + \frac{Gh^3}{12}\frac{\partial N_i}{\partial y}\frac{\partial N_j}{\partial y} + G\hat{k}h\, N_i N_j\right) dxdy$$

$$K_{ij}^{23} = \iint_A \left(\nu D\frac{\partial N_i}{\partial x}\frac{\partial N_j}{\partial y} + \frac{Gh^3}{12}\frac{\partial N_i}{\partial y}\frac{\partial N_j}{\partial x}\right) dxdy$$

$$G_{ij}^{11} = \iint_A \left[n_x^{(0)}\left(\frac{\partial N_i}{\partial x}\frac{\partial N_j}{\partial x}\right) + n_y^{(0)}\left(\frac{\partial N_i}{\partial y}\frac{\partial N_j}{\partial y}\right) + n_{xy}^{(0)}\left(\frac{\partial N_i}{\partial x}\frac{\partial N}{\partial y} + n_{xy}^{(0)}\left(\frac{\partial N_i}{\partial y}\frac{\partial N_j}{\partial x}\right)\right] dxdy$$

$$G_{ij}^{22} = \frac{h^2}{12}\iint_A \left[n_x^{(0)}\left(\frac{\partial N_i}{\partial x}\frac{\partial N_j}{\partial x}\right) + n_y^{(0)}\left(\frac{\partial N_i}{\partial y}\frac{\partial N_j}{\partial y}\right) + n_{xy}^{(0)}\left(\frac{\partial N_i}{\partial x}\frac{\partial N}{\partial y} + n_{xy}^{(0)}\left(\frac{\partial N_i}{\partial y}\frac{\partial N_j}{\partial x}\right)\right] dxdy$$

$$G_{ij}^{33} = \frac{h^2}{12}\iint_A \left[n_x^{(0)}\left(\frac{\partial N_i}{\partial x}\frac{\partial N_j}{\partial x}\right) + n_y^{(0)}\left(\frac{\partial N_i}{\partial y}\frac{\partial N_j}{\partial y}\right) + n_{xy}^{(0)}\left(\frac{\partial N_i}{\partial x}\frac{\partial N_j}{\partial y}\right) + n_{xy}^{(0)}\left(\frac{\partial N_i}{\partial y}\frac{\partial N_j}{\partial x}\right)\right] dxdy$$

$$G_{ij}^{12} = G_{ij}^{13} = G_{ij}^{23} = 0$$

$$i = 1,2,\ldots n \qquad j = 1,2,\ldots n$$

where n is the number of nodes on each element. The $\hat{k}$ is the transverse shear correction factor (in this paper $\hat{k} = 5/6$, which was proposed by Reissner). Eq. (8) is the matrix equation for each element. After assembling the process, the global matrix equation can be written as follows:

$$([K] - \lambda_b[Kg])\{\delta\} = 0$$

$$[K] = [K_b] + [K_s] \tag{9}$$

where

$[K_b]$: global bending matrix

$[K_s]$: global transverse shear matrix

$[K_g]$: global stiffness matrix

$$\{\delta\} = \{\{w\}, \{\theta_x\}, \{\theta_y\}\}^T$$

Eq. (9) is an eigenvalue problem. Eigenvalues and eigenvectors can be solved numerically. Eigenvalue are the buckling parmeter λ_b. Critical buckling load can be calculated through λ_b.

Boundary Conditions

Different boundary conditions that are simply supported, clamped, and free are considered on both outside and inside edges. The abbreviated symbol *S-S* means both outside and inside edges are simply supported. The *C-F* means outside clamped and inside free. The *C-C* means outside clamped and inside clamped. The *S-F* means outside simply supported and inside free. Biaxial symmetry is assumed for both geometry and loadings. Inside edges are not loaded, but boundary conditions were specified. The opening ratio is defined as A'/A (cut out area/whole area).

Simply Supported

$$w = 0,\ \theta_y = 0 \quad \text{along } x = a$$

$$w = 0,\ \theta_x = 0 \quad \text{along } y = a$$

$$\theta_x = 0 \quad \text{along } x = 0$$

$$\theta_y = 0 \quad \text{along } y = 0$$

Clamped

$$w = 0,\ \theta_x = 0,\ \theta_y = 0 \quad \text{along } x = a$$

$$w = 0,\ \theta_x = 0,\ \theta_y = 0 \quad \text{along } y = a$$

$$\theta_x = 0 \quad \text{along } x = 0$$

$$\theta y = 0 \quad \text{along } y = 0$$

Free End

At free end, w, θ_x, and θ_y are treated as unknowns. Typical mesh are shown in Fig. 4.

Numerical Technique

The Gauss-Legendre quadrature is used for numerical integration. Subspace iteration is used for solving eigenvalues and the eigenvector. Subspace iteration is known for its ability to handle a large dimension matrix.[11]

When span ratio (b/h) increases (approaches thin plate), the Mindlin's thick-plate theory suffers a phenomenon called

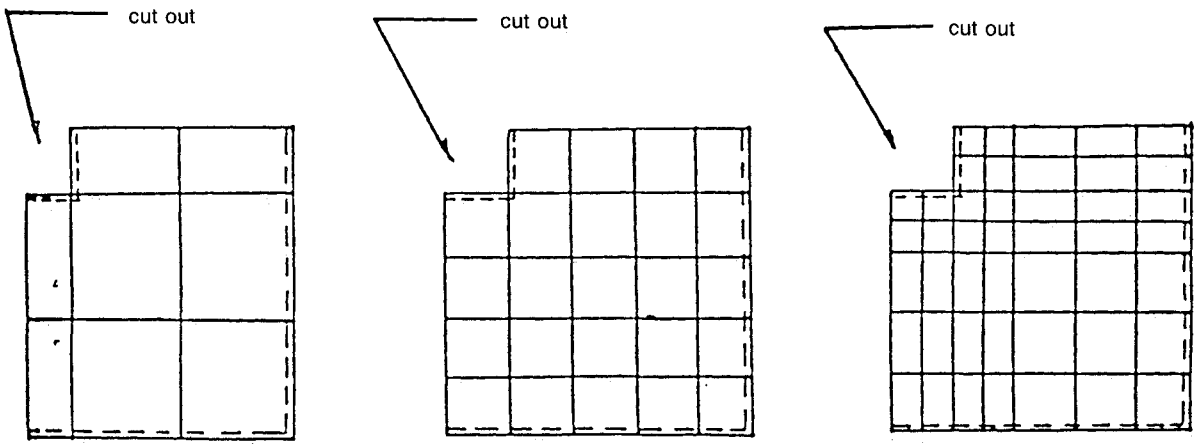

Fig. 4 Typical finite element meshes.

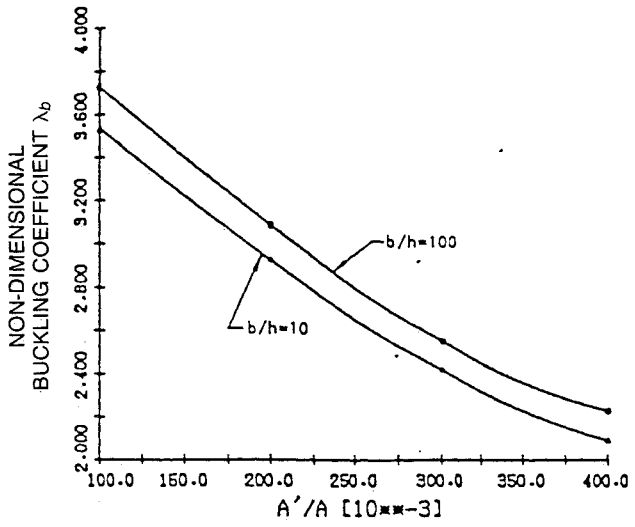

Fig. 5 Buckling parameter vs opening ratio (single axis prestressed, *S-F* boundary.

Table 1 Gauss point for regular and reduced integration

	Regular		Selective	
Element	K_b	K_s	K_b	K_s
4 nodes	2 × 2	2 × 2	2 × 2	2 × 1
8 nodes	3 × 3	3 × 3	3 × 3	2 × 2

"Locking."[12] To reduce locking, the transverse shear part of the stiffness matrix is reduced by using the "reduced integration technique."[13]

The use of the Gauss-Legendre quadrature in this study is illustrated as follows. For a rectangular domain, let

$$I = \int_{-1}^{1}\int_{-1}^{1} F(\xi,\eta)\, d\xi d\eta$$

Then

$$\int_{-1}^{1} F(\xi,\eta)\, d\xi = \sum_{j=1}^{r} W_j F(\xi_j,\eta) = \Psi(\eta)$$

$$I = \int_{-1}^{1} \Psi(\eta)\, d\eta = \sum_{i=1}^{r} W_i \Psi(\eta_i)$$

$$= \sum_{i=1}^{r} W_i \sum_{j=1}^{r} W_j F(\xi_j,\eta_i)$$

$$= \sum_{i=1}^{r}\sum_{j=1}^{r} W_i W_j F(\xi_j,\eta_i)$$

where

W_i, W_j: weighting factor

ξ_i, η_i: Gauss points

r: number of Gauss points

If F is a polynomial, then τ is normally equal to $n/2$. If n is an odd number, then r is rounded to the larger integer. Reduced integration[14] selects less Gauss points than regular Gauss integration. Selective, reduced integration partly uses regular and partly uses reduced Gauss integration. For the

Table 2 Validity checkout for full plate buckling, *EX*: full integration, SR: selective reduced integration

Boundary condition	4 sides simply supported single axis prestressed				4 edges clamped single axis prestressed		4 edges clamped single axis prestressed
b/h	100		10		100		100
Element No.	16	25	16	25	16	25	25
Node No.	65	96	65	96	65	96	96
Total D.O.F.	195	288	195	288	195	288	288
λ_b EX	4.0296	4.0152	3.8367	3.8344	10.975	10.4960	2.0076
λ_b % error	0.74	0.38	0.256	0.250	8.990	4.230	0.380
λ_b SR	—	3.9998	—	3.8382	—	10.1010	—
λ_b % error	—	0.005	—	2.450	—	0.300	—
λ_b (analytical)	4.000		3.741		10.070		2.000

Table 3 Buckling parameter λ_b for *S-F* boundary, $b/h = 100$, single-axis prestressed

A'/A	0.1		0.2		0.3		0.4	
Element No.	24	45	24	45	24	45	24	45
Node No.	93	164	93	164	93	164	93	164
Total D.O.F.	279	492	279	492	279	492	279	492
λ_b	3.7731	3.7307	3.1718	3.0813	2.6154	2.5504	2.2294	2.2177

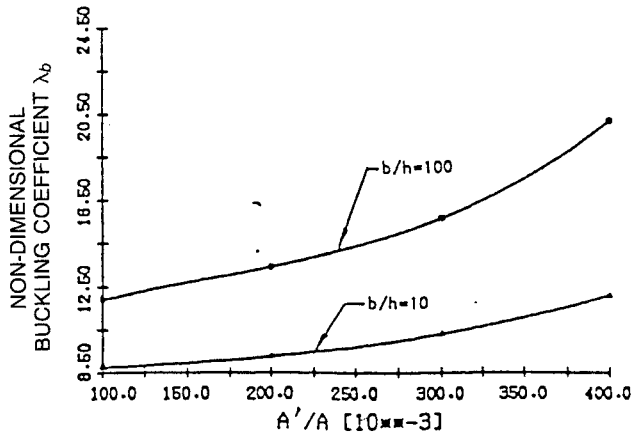

Fig. 6 Buckling parameter vs opening ratio (single axis prestressed, *S-S* boundary).

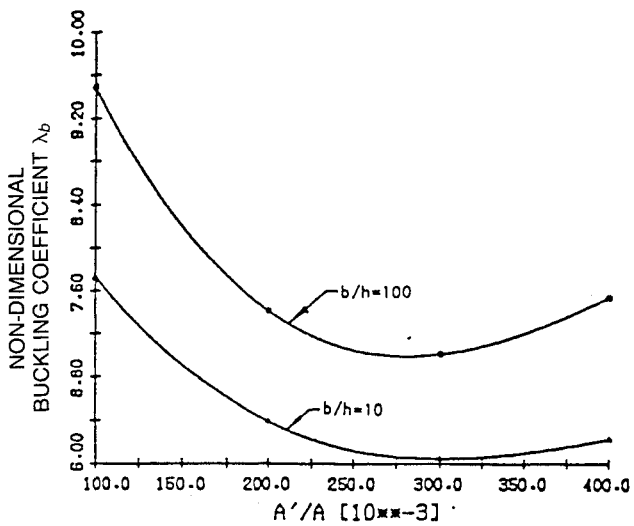

Fig. 7 Buckling parameter vs opening ratio (single axis prestressed, *C-F* boundary).

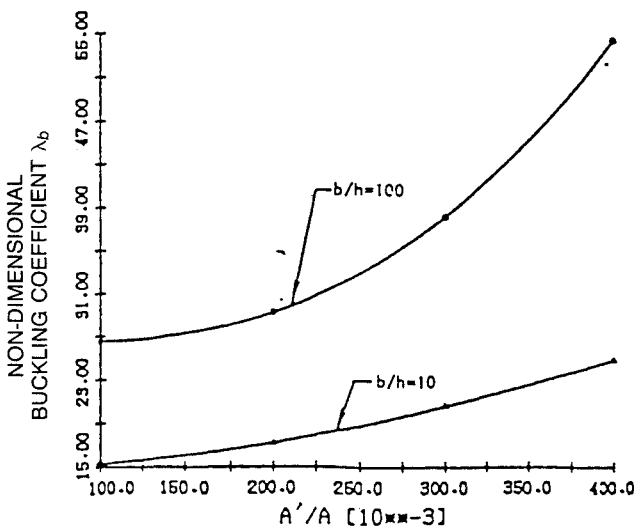

Fig. 8 Buckling parameter vs opening ratio (single axis prestressed, *C-C* boundary).

current study, the stiffness matrix of the transverse, shear term adapted reduced Gauss points, and the bending-stiffness term used regular Gauss points. Table 1 shows the number of Gauss points used for different cases. Where K_b is the stiffness matrix due to bending, and K_s is the stiffness matrix due to transverse shear.

Results and Discussions

The validity of the computation was checked out against the work of Srinivas[15] and Timoshenko[16] for full-plate buckling. comparisons are shown in Table 2. Excellent agreements are obtained. Numerical convergence of the plates with interior cutout were also examined with respect to the element numbers. A typical case (*B-F* boundary) is shown in Table 3. The

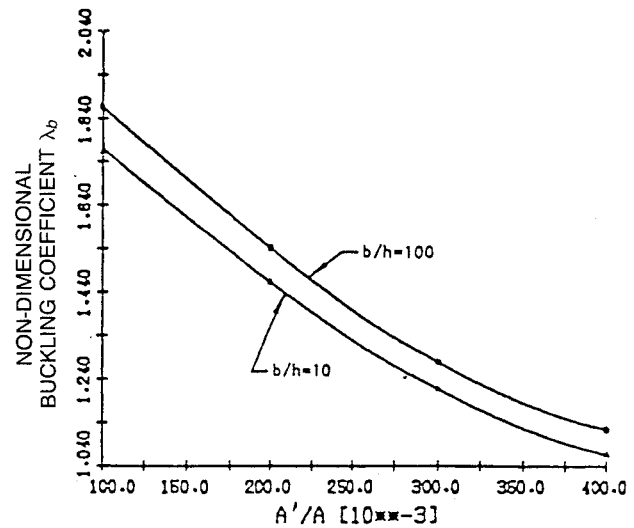

Fig. 9 Buckling parameter vs opening ratio (double axis prestressed, *S-F* boundary).

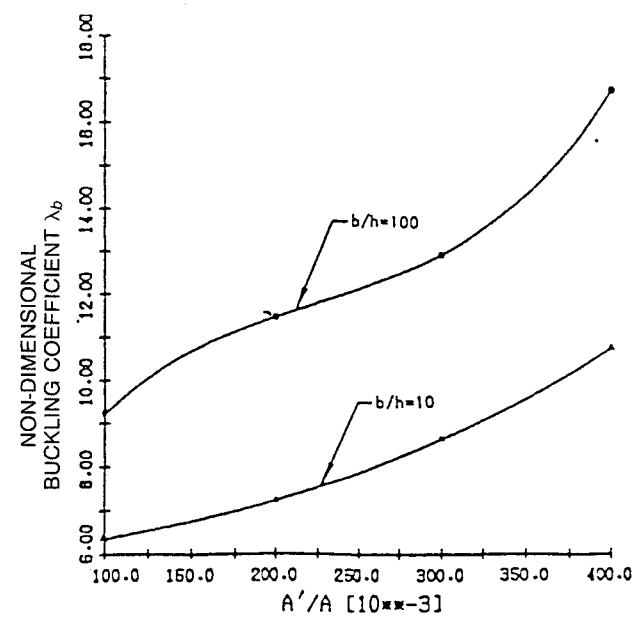

Fig. 10 Buckling parameter vs opening ratio (double axis prestressed, *S-F* boundary).

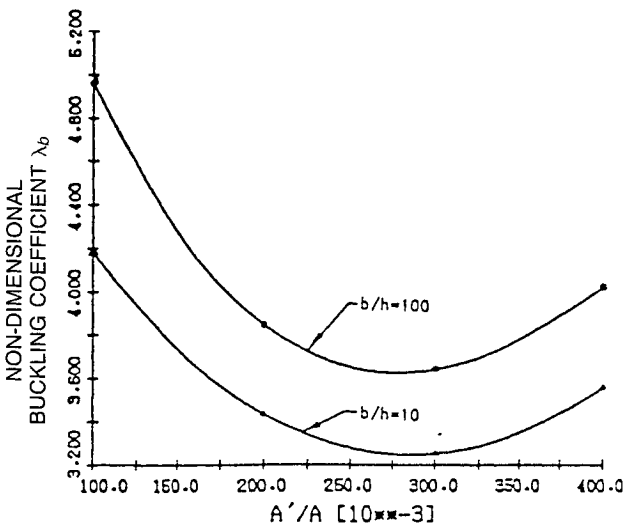

Fig. 11 Buckling parameter vs opening ratio (double axis prestressed, *C-F* boundary).

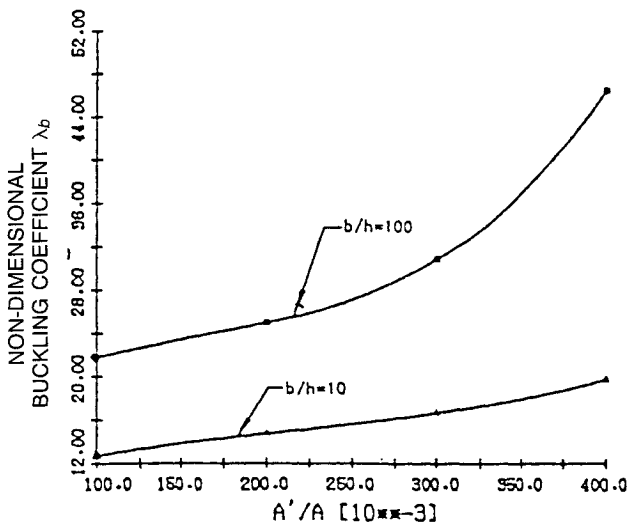

Fig. 12 Buckling parameter vs opening ratio (double axis prestressed, *C-C* boundary).

maximum element number used is 45. General convergent situations are quite good.

Figures 5–12 plot the λ_b vs the opening ratio A/A' (cutout area/whole area) for various boundaries and two prestressed conditons. The opening ratio appears to have significant effects on the buckling for all the cases studied.

For *S-F* boundary, λ_b decreases rapidly when A/A' increases (see Fig. 5). This simply means that the plate structures are substantially weakened by interior cutout. For *S-S* and *C-C* boundaries, λ_b increases w.r.t. A'/A (Figs. 6 and 8). It seems that the interior edges constraint stiffened the structures. Compare constrained and free interior edges (*S-F, C-F, S-S, C-C*). It is noted that λ_b for the constraint interior edges is about one order higher than free interior cases. For the *C-F* boundary, λ_b picks a minimum value around $A'/A = 0.27$ (see Fig. 7). This is a rather peculiar phenomenon. The authors have no handy theoretical explanation. Theoretical or experimental verifications would be very helpful.

The effect of transverse shear appears to become more significant when interior cutout increases for clamped and simply supported interior edges. This phenomenon can be observed from the fact that vertical distance between the two curves ($b/h = 10,100$) increases for larger A'/A (see Figs. 6, 8, 10, and 12). No such phenomenon is observed for free interior edges. This seems consistent with the assumption that zero-transverse, shear stress exists at free boundaries.

In summary, buckling of plates with interior cutout is important for safe engineering design. The current research offers useful information for designers.

Acknowledgment

The authors wish to thank the National Science Council in Taiwan for sponsoring this research project (Project NSC76-0401-E008-01).

References

[1]Sun, C. T., "On Equations for Timoshenko Beam Under Initial Stress," *Journal of Applied Mechanics*, Vol. 37, March 1972, pp. 282–285.

[2]Brunelle, E. J., "Stability and Vibration of Transversely Isotropic Beams Under Initial Stress," *Journal of Applied Mechanics*, Vol. 37, Sept. 1972, pp. 819–821.

[3]Herrmann, G., and Armenakas, A. E., "Vibration and Stability of Plates Under Initial Stress," *Journal of Engineering Mechanics*, ASCE, Vol. 86, No. EM3, June 1960, pp. 65–94.

[4]Burnelle, E. J., and Robertson, S. R., "Initially Stressed Mindlin Plates," *AIAA Journal*, Vol. 12, No. 8, 1974, pp. 1036–1045.

[5]Hinton, E., "Buckling of Initially Stressed Mindlin Plates Using a Finite Strip Method," *Computers and Structures*, Vol. 8, 1978, pp. 99–105.

[6]Dawe, D. J., and Roufaeil, O. L., "Buckling of Rectangular Mindlin Plates," *Computers and Structures*, Vol. 15, No. 4, 1982, pp. 461–471.

[7]Cheung, Y. K., Chan, H. C., and Tham, L. G., "A Study on the Linear Elastic Stability of Mindlin Plates," *International Journal for Numerical Methods in Engineering*, Vol. 22, No. 1-3, 1986, pp. 117–132.

[8]Paramasivam, P., Jawalker, K., and Rao, S., "Buckling of Plates of Abruptly Varying Stiffnesses," *Journal of the Structural Division*, ASCE ST6, June 1969, pp. 1313–1337.

[9]Mizusawa, T., Kajita, T., and Nuruoka, M., "Vibration and Buckling Analysis of Plates of Abruptly Varying Stiffness," *Computers and Structures*, Vol. 12, 1980, pp. 689–693.

[10]Tham, L. G., Chan, A. H. C., and Cheung, Y. K., "Free Vibration and Buckling Analysis of Plates by the Negative Stiffness Method," *Computers and Structures*, Vol. 22, No. 4, 1986, pp. 687–692.

[11]Bathe, K. J., *Finite Element Procedures in Engineering Analysis*, Prentice-Hall, Englewood Cliffs, NJ, 1981.

[12]Tsach, U., "Locking of Thin Plate/Shell Elements," *International Journal for Numerical Methods in Engineering*, Vol. 17, No. 1-6, 1981, pp. 633–644.

[13]Hughes, T. J. R., Cohen, M., and Haroun, M., "Reduced and Selective Integration Techniques in the Finite Element Analysis of Plates," *Nuclear Engineering and Design*, Vol. 46, 1978, pp. 203–222.

[14]Pugh, E. D. L., Hinton, E., and Zienkiewicz, O. C., "A Study of Quadrilateral Plate Bending Elements with Reduced Integration," *International Journal for Numerical Methods in Engineering*, Vol. 12, 1978, pp. 1059–1079.

[15]Srinivas, S., and Rao, A. K., "Buckling of Thick Rectangular Plates," *AIAA Journal*, Vol. 7, No. 8, 1969, pp. 1645–1646.

[16]Timoshenko, S. P., and Gere, J. M., "Theory of Elastic Stability," 2nd ed., McGraw-Hill, New York, 1961.